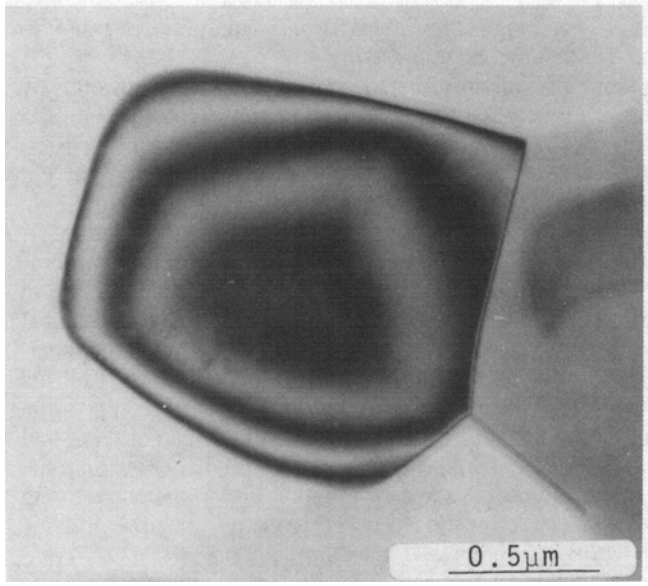

Fig. 7—Microstructure of 78.2 pct Zn-Al ice-water quenched and deformed 10 pct in tension at room temperature. TEM 200 kv.

absence of slip bands on the surface. The dislocation's density was observed to be the same before and after deformation (10^3 dislocations/cm^2). The grains remain equiaxed and of the same size after deformation (Figure 7).

It seems to be that deformation of these alloys at room temperature takes place by grain boundary sliding as they do at high temperature. Fracture at room temperature inhibits further deformation.

One approach to explain the substantial difference between the yield stresses of the ice-water quenched material, when tested in compression or tension, is to consider that the shear stress for one grain to glide over another consists of two components: one is the shear stress (τ_c) required to overcome the cohesion between grains, and the other is a frictional strength (μ) which is proportional to the normal stress (σ_n) on the shear plane. Thus, we may write $\tau = \tau_c + \mu\sigma_n$.

The term $\mu\sigma_n$ is expected to be bigger in compression than in tension. When the material is tested in compression, there is a compressive normal stress (σ_n) on the shear plane that increases the "packing" of the grains, increasing the friction. The bigger the friction, the more difficult it is for them to slide over one another. In tension this normal component of the stress is going to work in the reverse way, reducing the friction.

The pearlite structure is not very sensitive to this "packing effect" because it is composed of "flakes" instead of grains, so its yield stress in compression is almost the same as in tension.

This work was partially supported by the Organization of the American States. We thank Dr. T. G. Langdon for his critical review of this paper.

REFERENCES

1. J. W. Edington, K. N. Melton, and C. P. Cutler: *Progr. Mater. Sci.*, 1976, vol. 21, pp. 61-170.
2. D. M. R. Taplin, G. L. Dunlop, and T. G. Langdon: *Ann. Rev. Mater. Sci.*, 1979, vol. 9, pp. 151-89.
3. F. A. Shunk: *Constitution of Binary Alloys*, 2nd Supplement, McGraw-Hill, 1969.
4. L. F. Mondolfo: *Aluminum Alloys*, Butterworths, 1976, p. 400.
5. Fu-Wen Ling and David E. Laughlin: *Metall. Trans. A*, 1979, vol. 10A, pp. 921-28.
6. L. Valdés, J. Negrete, and G. Torres-Villaseñor: Proceedings of the "VI Congreso de la Academia Nacional de Ingeniería", Querétaro, Qro. México, 1980, pp. 284-88.

Fractographic Observations of Cleavage Initiation in the Ductile-Brittle Transition Region of a Reactor-Pressure-Vessel Steel

A. R. ROSENFIELD, D. K. SHETTY, and A. J. SKIDMORE

Unstable cleavage fracture of steels in the lower-shelf region is generally viewed as a process governed by a critical value (σ_f^*) for the maximum tensile stress (σ_{yy}). Micromechanisms postulated for cleavage crack initiation and extension include cracking of grain-boundary carbides by slip or twinning and critical extension of these carbide cracks into the adjoining ferrite grain.[1] It has generally been found that the critical tensile stress, σ_f^*, is independent of temperature and strain rate when carbide-crack nucleation is slip-induced.[2] These results and an additional postulate that σ_{yy} must exceed σ_f^* over a "characteristic microstructural dimension" ahead of a precrack are the bases of the Ritchie, Knott, and Rice[3] model for temperature and strain-rate dependence of fracture toughness (K_{Ic}) in the lower-shelf region. The model has since been extended and applied to nuclear pressure vessel steels[4] as well as other steels.[5]

In the ductile-brittle transition region unstable cleavage fracture can occur after variable amounts of stable crack growth by the dimple-rupture mechanism. This, in turn, is reflected in large scatter in the measured values of K_{Ic}, and determination of a lower-bound fracture toughness for use in safety analysis becomes a significant practical problem.[6] Apart from these practical considerations the micromechanism of cleavage initiation in the ductile-brittle transition region is intriguing because its occurrence in conjunction with the higher-energy ductile-rupture mechanism implies that cleavage-triggering is a stochastic process that must be treated in statistical terms including a consideration of the microstructural features necessary for cleavage nucleation. A statistical approach to the cleavage fracture of steels was suggested by the work of Hahn *et al.*[7] and has been reconsidered in a number of recent studies.[8-12]

The purpose of this note is to report the results of a fractographic study conducted on a group of 1T compact

A. R. ROSENFIELD, Research Leader, D. K. SHETTY, Principal Research Scientist, and A. J. SKIDMORE, Electron Metallographic Specialist, are all with Battelle–Columbus Laboratories, 505 King Avenue, Columbus, OH 43201.

Manuscript submitted February 14, 1983.

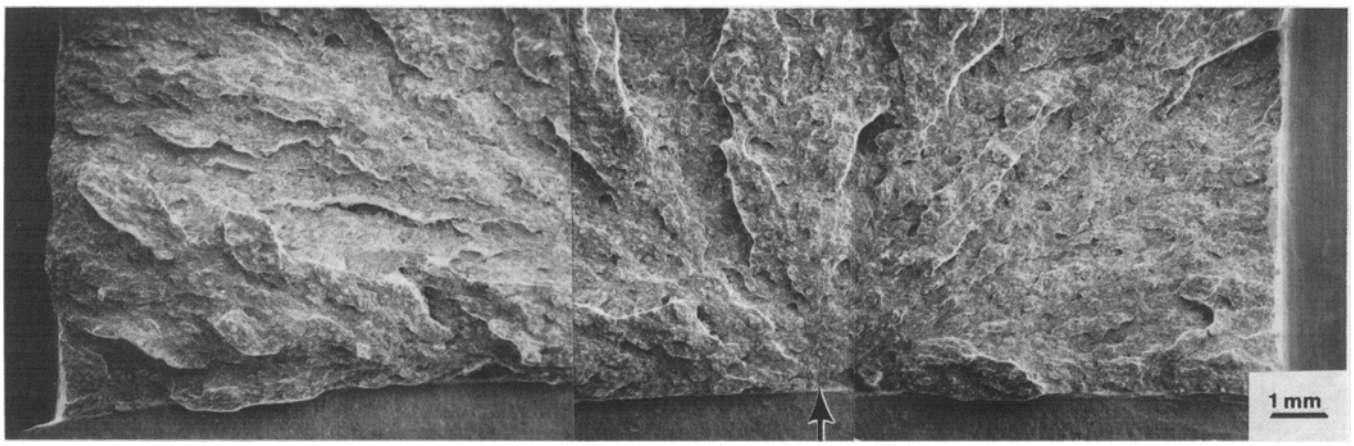

Fig. 1 — Fracture surface of a 1T compact specimen (T6-109) tested at 82 °C and rapid loading rate (550 mm/s). Arrow indicates the location of cleavage initiation.

fracture toughness specimens of a heavy-section A508 steel denoted TSE6[13] tested in the ductile-brittle transition region (22 and 82 °C). The fatigue-precracked specimens were loaded at a rapid rate (760 or 550 mm per second) to promote cleavage-crack growth and lower-bound toughness behavior. All specimens experienced unstable cleavage fracture prior to reaching a maximum in the load displacement curve. Some ductile crack growth occurred in half of the specimens.

The objective of the fractographic examinations was to understand the observed statistical variations in cleavage initiation by (a) locating the origins of unstable cleavage fracture in the vicinity of the fatigue-precrack or ductile-rupture crack fronts, (b) identifying microstructural features associated with the triggering of cleavage, and (c) documenting characteristic fracture surface dimensions such as the extent of stable-crack growth prior to unstable cleavage (Δa) and the distance of the cleavage origin from the ductile-rupture front, x (or fatigue-crack front when $\Delta a = 0$).

Twelve specimens, six each tested at the two temperatures, were examined by scanning electron fractography. In all but one of the specimens distinct cleavage fracture origins could be located near the fatigue or ductile-rupture crack fronts with the aid of directional fracture features. At low magnifications (~10×) the directional features included "tear ridges", *i.e.*, severely deformed ledges, nearly perpendicular to the fracture surface and linking two adjacent nonplanar cleavage surfaces. The tear ridges usually appeared as bright streaks on scanning electron fractographs as shown by the example of Figure 1 which shows fracture surface of a 1T compact specimen near the fatigue-crack front. The arrow indicates the general location of cleavage initiation. The fracture surface near the cleavage initiation region was then examined at successively higher magnifications. At intermediate magnifications (~100×) the cleavage-initiation region usually showed several ferrite grains with their cleavage facets nearly coplanar and parallel to the fatigue-crack plane (Figure 2). About half of the cleavage origins could be located within one of the ferrite grains. The circle in Figure 2 points out this cleavage-initiating grain in Specimen T6-109. The selection of the cleavage-initiating grain was made by following the "river patterns" on the cleavage facets of the coplanar ferrite grains. This selection was particularly easy in those cases

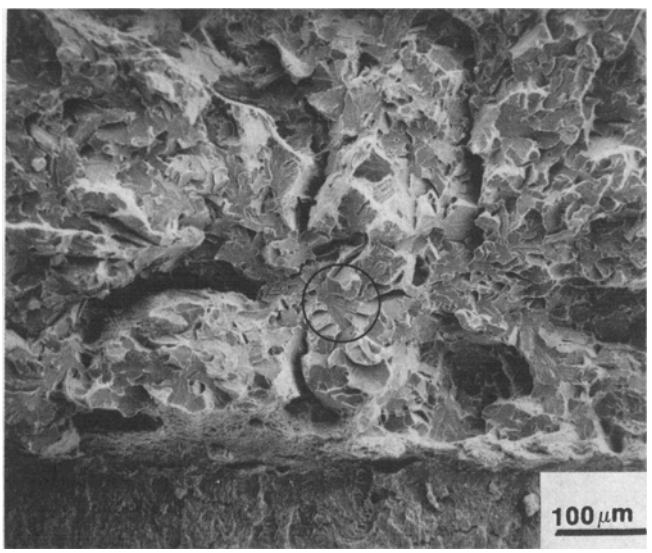

Fig. 2 — Cleavage-fracture origin ahead of fatigue and ductile crack front in specimen T6-109. Suspected origin is at the center of the circle.

where cleavage initiated from within a grain and the cleavage facet showed distinct "radial pattern" (Figure 3). In all cases of cleavage origin within a grain, the inclusion initiating cleavage was MnS. In other cases where cleavage initiated at a grain-boundary site, as shown by the example of Figure 4, cleavage is assumed to have been triggered by a carbide particle although the actual carbide particles were never observed. They were presumably dislodged during the rapid fracture event. In the case of MnS-initiated cleavage origins the sulfide particles were observed in approximately half of them. EDAX analysis was used on several origins and revealed either that particles were MnS or that the holes had high local concentrations of Mn and S.

Table I summarizes the fractographic observations on the 12 1T compact specimens. Included in the table are fracture toughness, K_{QJ}, calculated from the total area under the load-displacement curve, stable-crack growth by dimple rupture, Δa, measured in the vicinity of the cleavage origins, the number of cleavage origins in each specimen, the location of the cleavage origin ahead of the stable-crack front, x, and the cleavage-triggering inclusion whenever

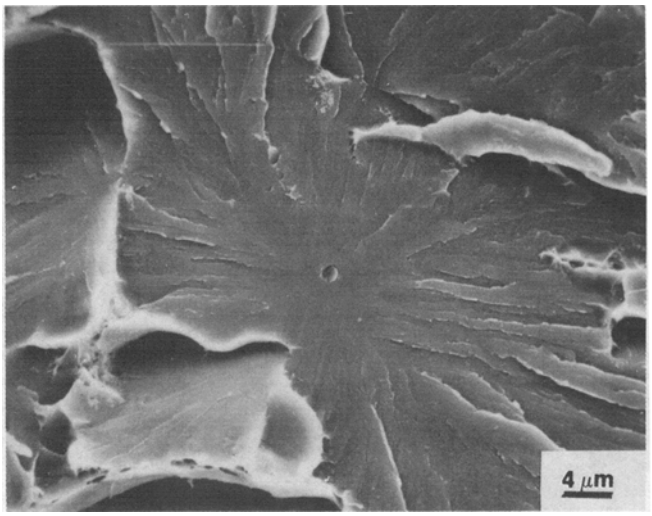

Fig. 3—Cleavage-triggering MnS inclusion (~1 μm) at the center of a ferrite grain in specimen T6-109.

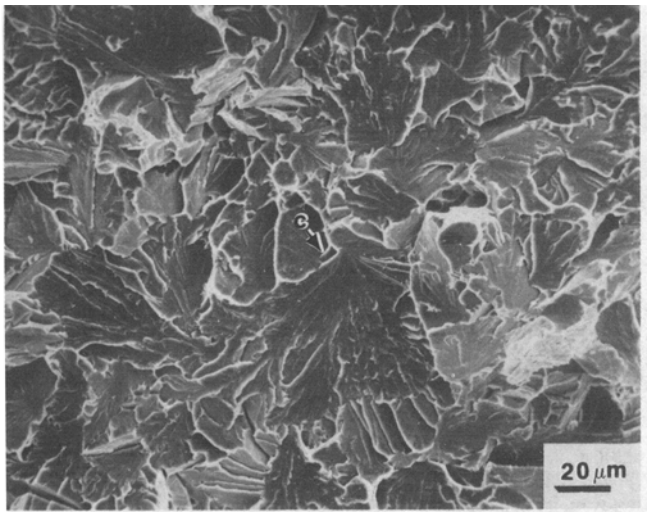

Fig. 4—Cleavage origin at a grain boundary site in specimen 90-2. C indicates the suspected site of crack-initiating carbide particle.

Table I. Summary of Fractographic Measurements on Rapidly-Loaded Precracked 1T Compact Specimens of TSE-6 Steel

Specimen	Test Temperature, C	K_{QJ}, MPa $m^{1/2}$	Stable Crack Growth (Δa), mm	No. of Cleavage Origins	Cleavage Origin Location (x), mm	Cleavage-Triggering Inclusion
90-2	22	180	0.05	1	1.74	g.b.c.*
86-1	22	86	0	1	0	u**
101	22	133	0	3	0.1, 0.1, 0.15	u, u, g.b.c.
102	22	103	0	1	0	u
103	22	116	0	3	0.07, 0.08, 0	u, u, MnS
104	22	84	0	Cleavage origin could not be identified		
90-1	83	276	0.6 to 0.7	2	2.0, 0.7	MnS, MnS
105	82	293	0.7	1	1.1	MnS
106	82	293	0.8	1	1.25	u
107	82	235	0.3	1	0.3	MnS
108	82	131	0	1	~0	u
109	82	217	0.08	1	0.175	MnS

*Grain-boundary carbide
u** Cleavage-triggering inclusion could not be identified but most of these origins were located at grain boundaries.

it was identified. The majority of the specimens showed single, well defined cleavage origins; three specimens showed multiple origins. There was no apparent correlation between fracture toughness and the number of cleavage origins. As might be expected, fracture toughness did increase with increasing amounts of stable-crack growth. A more interesting observation was that in specimens tested at the lower temperature and which showed no stable-crack growth ($\Delta a = 0$), fracture toughness appeared to correlate with the location of the cleavage origin relative to the fatigue-crack front; *i.e.*, K_{QJ} increased with increasing x. This observation is, of course, consistent with the concept of a critical value of tensile stress required to initiate cleavage in the stress field of a crack as discussed in the RKR model.[3] But the location of the cleavage origin (x) did not lend itself to any simple microstructural interpretation. The characteristic distance x varied anywhere from 0 up to 2 mm. For comparison, the largest microstructural features in this class of steel are local variations in hardness and grain size caused by carbon segregation. These variations reveal themselves as bands which are almost 1 mm in width.[14]

Two observations were unexpected in this study. A significant fraction of the cleavage fractures initiated at MnS inclusions of small size ~1 μm instead of at the carbides usually considered. Also, the MnS-triggered cleavage appeared to dominate the higher temperature tests where stable-crack growth occurred. The authors are not aware of any similar observations in any steels. However, Melander and Steninger[15] found that sulfides crack at considerably lower strains than does pearlite. If sulfides also crack more readily than grain boundary carbides in A508 steel they could serve as cleavage nuclei. But, this does not explain the observation that the microstructural features of the origins were not particularly unusual for the steel even though some cleavage origins were located as far away as 2 mm from the stable-crack fronts, and in some cases cleavage occurred only after significant amounts of stable-crack growth. It is now generally recognized, for example by Curry and Knott,[8] that the characteristic distance x must be viewed in statistical terms to account for the distribution of the critical microstructural dimensions, *viz.*, the thickness of the grain-boundary carbides. Our observations suggest that at least in

our quenched-and-tempered steels a secondary microstructural feature is more important in locating the cleavage origin or the so-called "weak spot". One tentative suggestion based on our fractography is that the secondary feature might be a collection of ferrite grains, possibly within the same prior-austenite grain, all of which have the same favorably oriented cleavage planes. A similar observation has been made by Ogawa *et al.*[14] Alternatively, the weak spots may be associated with the segregation bands. A more positive identification of the nature of the "weak spots" would be required, however, to understand fully the cleavage-triggering phenomenon and the associated scatter of fracture toughness of pressure-vessel steels in the ductile brittle transition region.

Note added in proof: Tweed and Knott[16] have recently reported cleavage being triggered by inclusions in C-Mn weld metal.

This research was supported by Oak Ridge National Laboratory under UCC-ND Subcontract 85X-13876C, as part of the HSST program sponsored by NRC. The continuing encouragement of G. D. Whitman, C. Pugh, and M. Vagins is gratefully acknowledged.

REFERENCES

1. E. Smith: Proc. Conf. "Physical Basis of Yield and Fracture", A. C. Strickland, ed., Oxford (Inst. Phys. and Phys. Soc.), 1966, pp. 36-46.
2. J. F. Knott: *J. Iron Steel Inst.*, 1966, vol. 204, pp. 104-11.
3. R. O. Ritchie, J. F. Knott, and J. R. Rice: *J. Mech. Phys. Solids*, 1973, vol. 21, pp. 395-410.
4. R. O. Ritchie, W. L. Server, and R. A. Wullaert: *Metall. Trans. A*, 1979, vol. 10A, pp. 1557-70.
5. D. A. Curry: *Mat. Sci. and Engg.*, 1980, vol. 43, pp. 135-44.
6. A. R. Rosenfield and D. K. Shetty: *Engg. Frac. Mech.*, 1981, vol. 14, pp. 833-42.
7. G. T. Hahn, R. G. Hoagland, and A. R. Rosenfield: *Metall. Trans.*, 1971, vol. 2, pp. 537-41.
8. D. A. Curry and J. F. Knott: *Metal Science*, 1979, vol. 13, pp. 341-45.
9. J. Landes and D. H. Shaffer: *Fracture Mechanics*, ASTM STP 700, P. C. Paris, ed., 1980, pp. 368-82.
10. A. R. Rosenfield and D. K. Shetty: *Engg. Frac. Mech.*, 1983, vol. 17, pp. 461-70.
11. A. G. Evans (U. Cal., Berkeley) and J. W. Hutchinson (Harvard): unpublished research, 1982.
12. A. Pineau: *Advances in Fracture Research*, D. Francois, ed., Pergamon (Oxford), 1981, vol. 2, pp. 553-77.
13. R. D. Cheverton, D. A. Canonico, S. K. Iskander, S. E. Bolt, P. P. Holz, R. K. Nanstad, and W. J. Stelzman: *Aspects of Fracture Mechanics on Pressure Vessels and Piping*, ASME Pub. PVP 58, 1982, pp. 1-15.
14. K. Ogawa, X. J. Zhang, T. Kobayashi, R. W. Armstrong, and G. R. Irwin: University of Maryland, College Park, MD, unpublished research, 1982.
15. A. Melander and J. Steninger: *Mat. Sci. Engg.*, 1982, vol. 52, pp. 239-48.
16. J. H. Tweed and J. F. Knott: *Metal Science*, 1983, vol. 17, pp. 45-54.